

Calorimetric evidence of multiband superconductivity in $\text{Ba}(\text{Fe}_{0.925}\text{Co}_{0.075})_2\text{As}_2$ single crystals

F. Hardy,^{1,*} T. Wolf,¹ R. A. Fisher,² R. Eder,¹ P. Schweiss,¹ P. Adelman,¹ H. v. Löhneysen,^{1,3} and C. Meingast¹

¹Karlsruher Institut für Technologie, Institut für Festkörperphysik, 76021 Karlsruhe, Germany

²Lawrence Berkeley National Laboratory, Berkeley, California 94720, USA

³Karlsruher Institut für Technologie, Physikalisches Institut, 76128 Karlsruhe, Germany

(Received 14 January 2010; published 3 February 2010)

We report on the determination of the electronic heat capacity of a slightly overdoped ($x=0.075$) $\text{Ba}(\text{Fe}_{1-x}\text{Co}_x)_2\text{As}_2$ single crystal with a T_c of 21.4 K. Our analysis of the temperature dependence of the superconducting-state specific heat provides strong evidence for a two-band s -wave order parameter with gap amplitudes $2\Delta_1(0)/k_B T_c=1.9$ and $2\Delta_2(0)/k_B T_c=4.4$.

DOI: [10.1103/PhysRevB.81.060501](https://doi.org/10.1103/PhysRevB.81.060501)

PACS number(s): 74.25.Bt, 65.40.Ba, 74.20.Rp, 74.70.Dd

The recently discovered iron arsenide family (FeAs) offers new possibilities for studying the interplay between superconductivity and magnetism.¹⁻³ As for many other materials, e.g., heavy fermions and cuprates, superconductivity emerges in the vicinity of a magnetic instability. The origin of the pairing interaction, as well as the gap symmetry, remains unidentified in the pnictides. Theoretically, the particular topology of the Fermi surface with strong nesting features favor a multiband order parameter having either an s_{\pm} -wave or a d -wave symmetry.⁴⁻⁷ In either case, a π -shift of the order-parameter phase is expected between different sheets of the Fermi surface. The identification of the gap symmetry is crucial, because it will shed light on the mechanism responsible for the condensation of Cooper pairs. Experimentally, solid evidence for a particular pairing state remains elusive, because several experimental probes point to different conclusions. For instance, in the electron-doped 122 compound, $\text{Ba}(\text{Fe}_{1-x}\text{Co}_x)_2\text{As}_2$, photoemission data (ARPES),⁸ and point-contact spectroscopy⁹ show two distinct nodeless gaps with large amplitudes, while penetration-depth measurements¹⁰ exhibit a power-law behavior reflecting the possible existence of nodes. Similar discrepancies are observed for hole-doped $(\text{Ba}_{1-x}\text{K}_x)\text{Fe}_2\text{As}_2$ and the 1111 series.^{11,12} Some of these apparent contradictions may arise from the influence of the magnetic instability, which is expected to strongly alter the gap topology,¹³ from impurity effects, or from experimental difficulties like sample inhomogeneities or surface off-stoichiometry. Specific-heat measurements can provide an important measure of the bulk superconducting properties; specifically, they can give valuable information about the possible existence of nodes in the energy gap and, as previously shown for MgB_2 ,^{14,15} to the number of bands that contribute to the superconducting condensate. Several specific-heat measurements have been reported for the Fe pnictides, but the interpretation of the results has been impaired by substantial contributions from paramagnetic centers and/or an incorrect evaluation of the large phonon background.^{11,16-18}

In this Rapid Communication, we present a detailed analysis of the electronic specific heat of a slightly overdoped $\text{Ba}(\text{Fe}_{1-x}\text{Co}_x)_2\text{As}_2$ single crystal with $x=0.075$, i.e., at a doping level where the static spin-density wave (SDW) is no longer observed. The problem of the phonon background determination is overcome by measuring a strongly overdoped crystal with $x=0.153$, in which superconductivity is

suppressed. Our analysis for the superconducting sample ($x=0.075$) gives strong evidence for two energy gaps, which implies that several sheets of the Fermi surface contribute to the formation of Cooper pairs. Additionally, we provide reliable values of the normal-state Sommerfeld coefficients $\gamma_n=C_e/T$ for several Co concentrations.

Co-doped Ba122 single crystals were grown from self-flux in glassy carbon crucibles. Prereacted FeAs and CoAs powders were mixed with Ba, placed into the crucible, which then was sealed in an evacuated SiO_2 ampoule. After heating to 650 °C and then to ≈ 1200 °C with holding times of 5 h, crystal growth took place during cooling at a rate of ≈ 1 °C/h. At 1000 °C, the ampoule was tilted to decant the remaining liquid flux from the crystals and subsequently removed from the furnace. The composition of these samples was determined by energy dispersive x-ray spectroscopy to be $x=0.075(\pm 0.005-0.01)$ and $x=0.153(\pm 0.005-0.01)$, respectively. The specific heat was measured with the ^3He option in a PPMS from Quantum Design.

Figure 1 shows the specific heat of both samples. No traces of a long-range SDW were detected for either sample in the entire temperature range, in agreement with previous

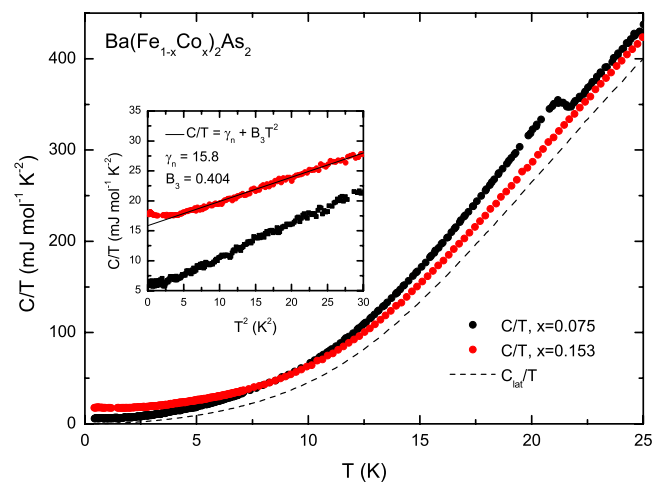


FIG. 1. (Color online) Temperature dependence of the specific heat C/T of samples with $x=0.075$ and $x=0.153$. The dashed line represents the lattice contribution, C_{lat}/T , derived from the specific heat for $x=0.153$ (see text). The inset shows the low-temperature specific heat of both samples.

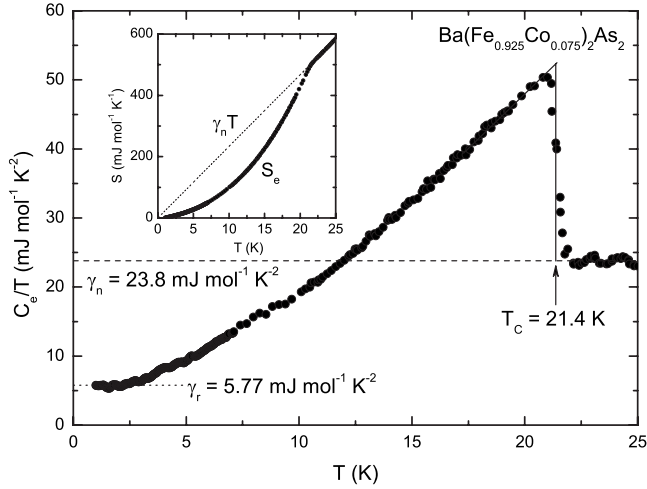


FIG. 2. Temperature dependence of the electron specific heat, C_e/T , of the superconducting sample ($x=0.075$). The dashed line represents the normal-state electron contribution, $\gamma_n=23.8 \text{ mJ mol}^{-1} \text{ K}^{-2}$. The dotted line is a residual normal-state-like contribution, $\gamma_r=5.77 \text{ mJ mol}^{-1} \text{ K}^{-2}$. The inset shows the normal- and superconducting-state electronic entropies.

reports.^{18–20} For $x=0.075$, a small anomaly at 21.4 K indicates the onset of bulk superconductivity. The second sample, with $x=0.153$, remains in the normal state down to 0.5 K, but its heat capacity exhibits an upturn below 2 K. Further measurements in magnetic fields have shown that this upturn is related to a Schottky-like contribution, probably due to paramagnetic centers which increase in number as the sample deteriorates in air. The specific heat of both samples is dominated by the lattice contribution; the electronic part is only about $\approx 15\%$ of the total signal at T_c , for $x=0.075$. Therefore, it is impossible to obtain an unequivocal lattice background by fitting the specific heat of the superconducting sample to an odd-power polynomial above T_c . Instead, a more reliable phonon term can be inferred from the data of the $x=0.153$ sample, whose low-temperature specific heat follows precisely the Debye law between 2 and 6 K, with $\gamma_n=15.8 \text{ mJ mol}^{-1} \text{ K}^{-2}$ and $B_3=0.404 \text{ mJ mol}^{-1} \text{ K}^{-4}$ (full line, inset of Fig. 1). Thus, an accurate lattice contribution C_{lat} is derived by combining the experimental data above 2 K with the fit extrapolation for $T < 2 \text{ K}$ (dashed line in Fig. 1), after subtraction of the electronic term.

Figure 2 shows the temperature dependence of the electron specific heat C_e ($x=0.075$) = $C(x=0.075) - f_s \cdot C_{lat}(x=0.153)$, with a scaling factor f_s of 1.01. The magnitude of f_s is determined by enforcing entropy conservation, i.e., $\int_0^{T_c} \gamma_n dT = \int_0^{T_c} C_e/T dT$ (inset of Fig. 2). The small deviation of f_s from unity, plausibly related to experimental uncertainties, demonstrates that the above procedure represents a very good method to determine the phonon background. Physically, this indicates that the substitution of Fe by Co does not substantially affect the lattice properties, as shown by recent inelastic x-ray scattering measurements and *ab initio* calculations.²¹

The superconducting transition at $T_c=21.4 \text{ K}$ is remarkably sharp, indicating little inhomogeneity in the crystal. The

TABLE I. Critical temperature (T_c) and normal-state electron specific heat (γ_n). Value for $x=0$ is taken from Ref. 22

x	T_c (K)	γ_n ($\text{mJ mol}^{-1} \text{ K}^{-2}$)
0	0	5.3
0.075	21.4	23.8
0.153	0	15.8

normal-state electron contribution for $x=0.075$ is $\gamma_n \approx 24 \text{ mJ mol}^{-1} \text{ K}^{-2}$, which is in excellent agreement with LDA+DMFT calculations, which require γ_n to be enhanced to 20–30 $\text{mJ mol}^{-1} \text{ K}^{-2}$ in order to explain mass renormalization by Hund coupling.²³ Our values for several Co concentrations, summarized in Table I, show that the disappearance of the SDW with Co doping is accompanied by an increase of the electronic density of states (EDOS), compatible with a progressive closure of the SDW gap. In the overdoped region, on the other hand, γ_n and T_c both decrease. Interestingly, γ_n of our superconducting sample is only about half as large as the value reported for K-doped 122 single crystals¹¹ ($\approx 63 \text{ mJ mol}^{-1} \text{ K}^{-2}$).

Figure 2 illustrates that C_e/T does not extrapolate to zero at $T=0$ but to a residual normal-state-like contribution $\gamma_r=5.8 \text{ mJ mol}^{-1} \text{ K}^{-2}$. Taken at face value, this would indicate that the sample has a superconducting fraction of $\approx 75\%$. Finite values of γ_r are a generic feature of specific-heat measurements of electron-doped 122 iron arsenides.^{11,24} For the cuprates,^{25,26} they have been attributed to an incomplete transition to the superconducting-state and volume fractions of normal and superconducting material γ_r/γ_n and $1 - \gamma_r/\gamma_n$, respectively. On this basis, the specific heat is the sum of separate contributions of the superconducting and normal phases and consequently, the electronic specific heat can be normalized to one mole of superconducting material, C_{es} , defined by:

$$C_{es} = (C_e - \gamma_r T) \frac{\gamma_n}{\gamma_n - \gamma_r}. \quad (1)$$

However, recent specific-heat²⁴ and heat-transport²⁷ measurements suggest that $\gamma_r T$ is a consequence of pair breaking in electron-doped 122 pnictides, and not due to the presence of normal material. In that case, the specific heat is, in principle, not the sum of contributions of broken pairs and the superconducting condensate. Nevertheless, in analogy with the Na cobaltates,²⁸ C_{es} (given by Eq. (1)) can be expected to be a reasonable and useful approximation to the specific heat of one mole of superconducting material, and is used, in Fig. 3, for the purpose of comparison with several possible order parameters. Figure 3(a) demonstrates that C_{es} cannot be described by the specific heat of a single-band BCS *s*-wave superconductor, calculated in the weak-coupling limit (blue line). The agreement is very poor. As for MgB_2 ,¹⁴ the positive curvature of C_{es} for $T/T_c > 0.6$, where the BCS curve shows negative curvature, is indicative of strong-coupling effects, but the observed discontinuity at T_c , $\Delta C_{es}/\gamma_n T_c$, which would be greater than the BCS value for a strong-

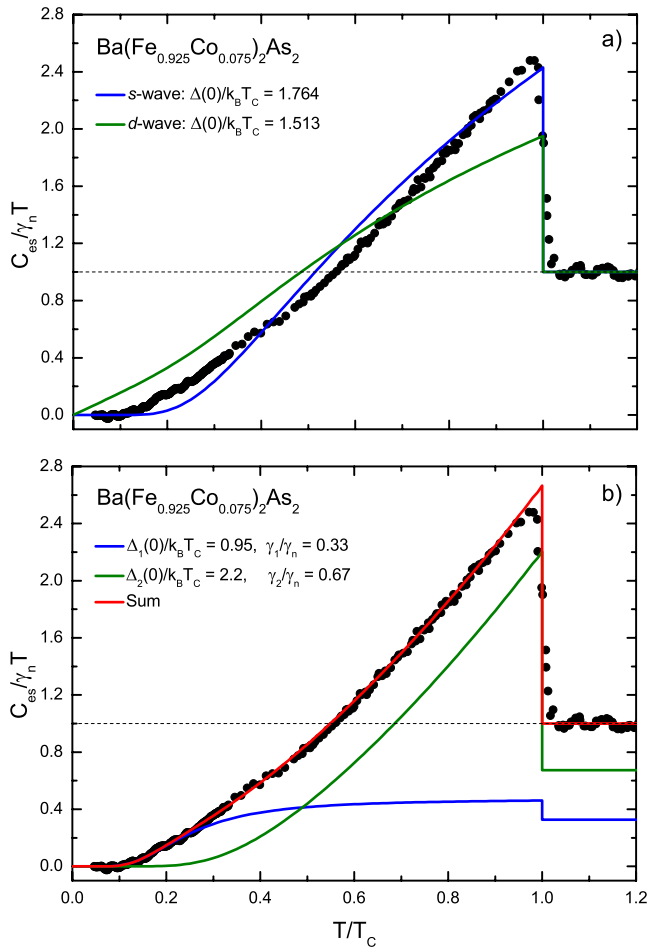


FIG. 3. (Color online) (a) The electron specific heat of the superconducting sample ($x=0.075$), normalized to 1 mol of superconducting condensate, compared with the specific heat of single-band s -wave (blue line) and d -wave (green line) order parameters, in the weak-coupling limit. (b) The electron specific heat of the superconducting sample ($x=0.075$), normalized to 1 mol of superconducting condensate. The red curve represents a two-gap fit. The blue and green curves are the partial specific-heat contributions of the two bands.

coupled single-band superconductor, is close to weak-coupling value. In addition, C_{es} is significantly larger than the BCS curve, for $T/T_c < 0.4$, again arguing against strong-coupling effects. Figure 3(a) also shows the specific heat of a single-band d -wave superconductor in the weak-coupling limit (green line).⁴¹ It is obvious that such a k -dependent gap, even in a strong coupling or a two-band scenario, cannot describe the observed low-temperature exponential behavior that can be inferred from the data.

We therefore focus our discussion on the possibility of two energy gaps, using the phenomenological two-band α -model, introduced by Bouquet *et al.*^{15,29} It allows a fit of the specific heat from low temperatures up to T_c and, as a result, gives reliable gap amplitudes that were shown to agree quantitatively with band calculations on MgB_2 in particular,^{15,30} and with Eliashberg equations in general.³¹ In this fit, the specific heat is taken as the sum of contributions from two bands, which are calculated independently assum-

TABLE II. Gap ratios $2\Delta_1(0)/k_B T_c$, $2\Delta_2(0)/k_B T_c$ and weights γ_1/γ_n as determined by the two-gap model and by different techniques.^{8,33,34}

Technique	x	$2\Delta_1(0)/k_B T_c$	$2\Delta_2(0)/k_B T_c$	γ_1/γ_n
$C(T)$	0.075	1.9	4.4	0.33
NMR	0.070	1.8	7.2	0.4
μSR	0.070	1.565	3.768	0.345
ARPES	0.075	4.1	6.4	

ing a BCS temperature dependence of the superconducting gaps. Two gap magnitudes, at $T=0$, are introduced as adjustable parameters, $\alpha_1 = \Delta_1(0)/k_B T_c$ and $\alpha_2 = \Delta_2(0)/k_B T_c$, together with a third quantity, γ_i/γ_n ($i=1,2$), which measures the fraction of the total normal EDOS that the i -th band contributes to the superconducting condensate.⁴² As shown in Fig. 3(b), the two-band fit (with $\alpha_1=0.95$, $\alpha_2=2.2$, and $\gamma_1/\gamma_n=0.33$) accurately reproduces the specific heat over the entire temperature range. These gap values conform to the theoretical constraints that one gap must be larger than the BCS gap and one smaller in a weakly coupled two-band superconductor.³² Moreover, they are comparable with those derived from recent NMR (Ref. 33) and μSR -penetration-depth measurements³⁴ (see Table II), but differ appreciably, by at least a factor 1.5, from ARPES data.⁸

$\text{Ba}(\text{Fe}_{0.925}\text{Co}_{0.075})_2\text{As}_2$ also shares similar properties with NbSe_2 , another candidate for multiband superconductivity, as illustrated by thermodynamic measurements^{35,36} and ARPES spectra.³⁷ The specific heat of both NbSe_2 and $\text{Ba}(\text{Fe}_{0.925}\text{Co}_{0.075})_2\text{As}_2$ show no sign of an incipient steep increase of $C(T)$ below T_c , which is the conspicuous signature of the small gap in MgB_2 .¹⁴ This increase is particularly pronounced in MgB_2 because (i) Δ_2/Δ_1 is about twice as large as in $\text{Ba}(\text{Fe}_{0.925}\text{Co}_{0.075})_2\text{As}_2$ and NbSe_2 , (ii) each gap gives an equal contribution, $\gamma_2/\gamma_1 \approx 1$, to the specific heat of MgB_2 . In contrast, in both NbSe_2 and $\text{Ba}(\text{Fe}_{0.925}\text{Co}_{0.075})_2\text{As}_2$ the major-gap contributions strongly dominate, with γ_2/γ_1 roughly equal to 4 and 2.3, respectively.

We now discuss to what extent our results are consistent with the predicted s_{+-} order parameter.⁴⁻⁷ In $\text{Ba}(\text{Fe}_{0.925}\text{Co}_{0.075})_2\text{As}_2$, the major gap develops around the Fermi-surface sheet that shows the largest EDOS, while it is theoretically expected that $\Delta_1/\Delta_2 \propto \sqrt{N_2/N_1}$, in the limit of pure interband pairing.³⁸ Our result is not incompatible with the s_{+-} -state, and could indicate that either intraband interactions are significant (as pointed out in Ref. 38), or that more than two bands are involved in the pairing mechanism.³⁹ The large residual EDOS observed in the superconducting state, in the present data, actually favors the s_{+-} -state, since non-magnetic scattering centers (e.g., Co dopant) are expected to be pair breaking for this particular state in the Born limit.^{6,40}

In summary, a detailed analysis of the electronic specific heat of $\text{Ba}(\text{Fe}_{0.925}\text{Co}_{0.075})_2\text{As}_2$ provides strong evidence of a multigap order parameter. Our data are fit very well by a two-band s -wave model. Further, we derive a reliable phonon contribution that permits to extract accurate values of the normal-state Sommerfeld coefficient.

*frederic.hardy@kit.edu

- ¹Y. Kamihara, T. Watanabe, M. Hirano, and H. Hosono, *J. Am. Chem. Soc.* **130**, 3296 (2008).
- ²M. Rotter, M. Pangerl, M. Tegel, and D. Johrendt, *Angew. Chem. Int. Ed.* **47**, 7949 (2008).
- ³A. S. Sefat, R. Jin, M. A. McGuire, B. C. Sales, D. J. Singh, and D. Mandrus, *Phys. Rev. Lett.* **101**, 117004 (2008).
- ⁴I. I. Mazin, D. J. Singh, M. D. Johannes, and M. H. Du, *Phys. Rev. Lett.* **101**, 057003 (2008).
- ⁵V. Cvetkovic and Z. Tesanovic, *EPL* **85**, 37002 (2009).
- ⁶K. Kuroki, S. Onari, R. Arita, H. Usui, Y. Tanaka, H. Kon-tani, and H. Aoki, *Phys. Rev. Lett.* **101**, 087004 (2008).
- ⁷Y. Bang and H.-Y. Choi, *Phys. Rev. B* **78**, 134523 (2008).
- ⁸K. Terashima *et al.*, *Proc. Natl. Acad. Sci. U.S.A.* **106**, 7330 (2009).
- ⁹P. Samuely, Z. Pribulová, P. Szabó, G. Pristáš, S. L. Bud'ko, and P. C. Canfield, *Physica C* **469**, 507 (2009).
- ¹⁰R. T. Gordon, C. Martin, H. Kim, N. Ni, M. A. Tanatar, J. Schmalian, I. I. Mazin, S. L. Bud'ko, P. C. Canfield, and R. Prozorov, *Phys. Rev. B* **79**, 100506(R) (2009).
- ¹¹G. Mu, H. Luo, Z. Wang, L. Shan, C. Ren, and H.-H. Wen, *Phys. Rev. B* **79**, 174501 (2009).
- ¹²C. Martin, R. T. Gordon, M. A. Tanatar, H. Kim, N. Ni, S. L. Bud'ko, P. C. Canfield, H. Luo, H. H. Wen, Z. Wang, A. B. Vorontsov, V. G. Kogan, and R. Prozorov, *Phys. Rev. B* **80**, 020501(R) (2009).
- ¹³D. Parker, M. G. Vavilov, A. V. Chubukov, and I. I. Mazin, *Phys. Rev. B* **80**, 100508(R) (2009).
- ¹⁴R. A. Fisher, G. Li, J. C. Lashley, F. Bouquet, N. E. Phillips, D. G. Hinks, J. D. Jorgensen, and G. W. Crab-tree, *Physica C* **385**, 180 (2003).
- ¹⁵F. Bouquet, Y. Wang, R. A. Fisher, D. G. Hinks, J. D. Jorgensen, A. Junod, and N. E. Phillips, *Europhys. Lett.* **56**, 856 (2001).
- ¹⁶U. Welp *et al.*, *Physica C* **469**, 575 (2009).
- ¹⁷L. Ding, C. He, J. K. Dong, T. Wu, R. H. Liu, X. H. Chen, and S. Y. Li, *Phys. Rev. B* **77**, 180510(R) (2008).
- ¹⁸S. L. Bud'ko, N. Ni, and P. C. Canfield, *Phys. Rev. B* **79**, 220516(R) (2009).
- ¹⁹J.-H. Chu, J. G. Analytis, C. Kucharczyk, and I. R. Fisher, *Phys. Rev. B* **79**, 014506 (2009).
- ²⁰N. Ni, M. E. Tillman, J.-Q. Yan, A. Kracher, S.-T. Han-nahs, S. L. Bud'ko, and P. C. Canfield, *Phys. Rev. B* **78**, 214515 (2008).
- ²¹D. Reznik *et al.*, *Phys. Rev. B* **80**, 214534 (2009).
- ²²F. Hardy (unpublished).
- ²³K. Haule and G. Kotliar, *Proceedings of the International Conference on Magnetism in Karlsruhe* (unpublished).
- ²⁴G. Mu, B. Zeng, P. Cheng, Z. Wang, L. Fang, B. Shen, L. Shan, C. Ren, and H. Wen, arXiv:0906.4513 (unpublished).
- ²⁵R. A. Fisher, B. Buffeteau, R. Calemczuk, K. W. Dennis, T. E. Hargreaves, C. Marcenat, R. W. McCallum, A. S. O'Connor, N. E. Phillips, and A. Schilling, *Phys. Rev. B* **61**, 1473 (2000).
- ²⁶A. Amato, R. A. Fisher, N. E. Phillips, and J. B. Torrance, *Physica B* **165-166**, 1337 (1990).
- ²⁷Y. Machida, K. Tomokuni, T. Isono, K. Izawa, Y. Naka-jima, and T. Tamegai, *J. Phys. Soc. Jpn.* **78**, 073705 (2009).
- ²⁸N. Oeschler, R. A. Fisher, N. E. Phillips, J. E. Gordon, M.-L. Foo, and R. J. Cava, *Phys. Rev. B* **78**, 054528 (2008).
- ²⁹H. Padamsee, J. E. Neighbor, and C. A. Shiffman, *J. Low Temp. Phys.* **12**, 387 (1973).
- ³⁰A. Y. Liu, I. I. Mazin, and J. Kortus, *Phys. Rev. Lett.* **87**, 087005 (2001).
- ³¹O. V. Dolgov, R. K. Kremer, J. Kortus, A. A. Golubov, and S. V. Shulga, *Phys. Rev. B* **72**, 024504 (2005).
- ³²V. Z. Kresin and S. A. Wolf, *Physica C* **169**, 476 (1990).
- ³³G. Q. Zheng, K. Matano, S. Kawasaki, Z. A. Ren, Z. X. Zhao, G. F. Chen, J. L. Luo, N. L. Wang, and C. T. Lin, *Proceedings of the International Conference on Magnetism in Karlsruhe* (unpublished).
- ³⁴T. J. Williams *et al.*, *Phys. Rev. B* **80**, 094501 (2009).
- ³⁵C. L. Huang, J.-Y. Lin, Y. T. Chang, C. P. Sun, H. Y. Shen, C. C. Chou, H. Berger, T. K. Lee, and H. D. Yang, *Phys. Rev. B* **76**, 212504 (2007).
- ³⁶E. Boaknin *et al.*, *Phys. Rev. Lett.* **90**, 117003 (2003).
- ³⁷T. Yokoya, T. Kiss, A. Chainani, S. Shin, M. Nohara, and H. Takagi, *Science* **294**, 2518 (2001).
- ³⁸O. V. Dolgov, I. I. Mazin, D. Parker, and A. A. Golubov, *Phys. Rev. B* **79**, 060502(R) (2009).
- ³⁹L. Benfatto, E. Cappelluti, and C. Castellani, *Phys. Rev. B* **80**, 214522 (2009).
- ⁴⁰A. A. Golubov and I. I. Mazin, *Phys. Rev. B* **55**, 15146 (1997).
- ⁴¹We assumed a cylindrical Fermi surface. For this geometry, $d_{x^2-y^2}$ and d_{xy} order parameters exhibit the same temperature-dependent specific heat.
- ⁴²with the constraint that $\gamma_1/\gamma_n + \gamma_2/\gamma_n = 1$.